ISSN 1063-780X, Plasma Physics Reports, 2025, Vol. 51, No. 7, pp. 842–853. © Pleiades Publishing, Ltd., 2025.

LOW-TEMPERATURE PLASMA

Evolution of Low-Frequency Barrier Discharge Plasma Radiation in Low-Pressure Neon. Ion Radiation Spectrum

V. A. Ivanov*

St. Petersburg State University, St. Petersburg, 199034 Russia

**e-mail: v.a.ivanov@spbu.ru*

Received April 11, 2025; revised June 20, 2025; accepted July 1, 2025

Abstract—Emission of low-frequency barrier discharge plasma in neon at a pressure of 1.4–1.7 Torr formed by transitions between excited states of the Ne^+ ion is studied in the wavelength range of 290–450 nm using kinetic spectroscopy methods. The difference in the relative intensities of ion lines at different stages of the plasma evolution is discussed: from direct excitation with ionization from the ground state of the atom by electron impact in the active stage (discharge), followed by a transition to the recombination afterglow as the electron temperature relaxes. The latter is due to the collisional-radiative recombination of doubly charged Ne^{2+} ions with electrons, creating at a density of the latter of $[e] \approx 10^{11}$ cm^{-3} the population flux of some Ne^{+}* levels comparable to excitation by electrons at the stage of the plasma creation. A significant number of ion lines corresponding to transitions from states with the principal quantum number $n = 3$ contain an intermediate stage, the explanation of which is based on the experimentally confirmed hypothesis that the long-lived neon atoms in metastable states participate in their excitation. In contrast, the spectral lines of transitions from excited states of the Ne^{+}* ion of $2s^2 2p^4 (^3P_2) 4f$ configurations do not have this stage.

Keywords: dielectric barrier discharge, ion lines, electron impact excitation, afterglow, collisional-radiative recombination

DOI: 10.1134/S1063780X25603220

1. INTRODUCTION

This work is a continuation of the experimental study [1, 2] of the emission spectrum of an extended low-frequency dielectric barrier discharge (DBD) of the cylindrical configuration in low-pressure neon. The active stage of such a discharge formed by two half-waves of the current with a duration of several microseconds of different polarities [3] creates plasma with a density of excited Ne^{+}* ions high enough for spectroscopic observations at gas pressures of a units–fractions of Torr [3, 4]. The formation of these ions also continues in the plasma deionization stage because of the collisional-radiative recombination of doubly charged Ne^{2+} ions with electrons [5, 6]. In contrast to [1] devoted to the description of the atomic spectrum, in this work, main attention is paid to the analysis of the excitation processes of ion levels in such plasma at different stages of its evolution.

The study of the spectra of atoms with low degrees of ionization has traditionally been carried out using a discharge with a hollow cathode made of various materials and filled with an inert gas as a radiation source. A detailed list of such studies, which have been begun in the 1930s [7], is contained in [8, 9]. These studies made the major contribution to the formation of the NIST database [10] on transitions in the Ne^{+}* ion.

In terms of the analysis of the excitation of ion (as well as atomic) levels by electrons, the issue of the competition between direct and stepwise excitation processes is important. Sufficiently high densities of ions (atoms) in long-lived metastable or resonance states are necessary for the latter to be implemented. Unlike the atomic spectra of all inert gases, the excitation of which in gas–discharge plasma is to a significant extent caused by a stepwise process, which, in particular, occurs at the initial stage of the decay of the barrier discharge plasma [1], the interpretation of the evolution of emission in the ion spectrum is more complicated [2]. According to the data of experiments, the results of which are sensitive to the presence of long-lived excited ions (e.g., [11]—the study of the electron yield during the interaction of ions with a metal surface; [12]—ionization in crossed electron–ion beams), Ne^{+}* ions have no states with radiation times significantly exceeding $\tau_{rad} \approx 10^{-5}$ s. Note that in the same experiments, metastable states of singly charged ions of heavy inert gases were discovered. These were the $^4D_{7/2}$, $^4F_{9/2}$, $^4F_{7/2}$, and $^2F_{7/2}$ states [11]. Multiply charged neon ions also have metastable states [13, 14]. The specificity of Ne^{+}* ions, apparently

caused by the complex nature of the interaction of spin and orbital moments of electrons, is manifested in a significantly deeper, compared to the atomic spectrum, "dip" in the intensities of the majority of ion lines $J_i(t)$ in the initial stage of the plasma decay separating the active stage from the afterglow associated with the collisional-radiative recombination of doubly charged ions with electrons. At the same time, as shown in [2], a significant fraction of ion lines in this intermediate stage $J_{int}(t)$ has a fairly bright glow, the intensity of which is independent of the plasma electron temperature. The explanation for this phenomenon in [2] is proposed to be sought in processes involving heavy plasma particles, which constituted one of the tasks of this work.

The mechanism of collisional-radiative recombination (CRR) of doubly charged ions

$$Ne^{++} + e + e \xrightarrow{\alpha_{2cr}} Ne^{+*} + e,$$

where α_{2cr} is the rate constant of the process, is of particular interest for the following reasons. Firstly, as a virtually unexplored source of the formation of excited particles in plasma, dramatically compacting its radiation spectrum especially in the near ultraviolet region [2, 3], which can be used to compare the collisional-radiative recombination rates of singly and doubly charged ions by kinetic spectroscopy methods [5, 6]. Secondly, as a process that significantly increases the plasma deionization rate, since its rate is many times higher than the decay rate of plasma with singly charged ions [6].

Finally, the interpretation of ionic luminescence in the active stage requires recourse to at least two mechanisms: direct excitation by electrons from the ground state of the neon atom and neon ion.

Thus, the aim of this work was to record the intensities of ion lines $J_i(t)$, emitted at different stages of the evolution of low-frequency barrier discharge plasma by excited levels of the Ne^{+*} ion with different excitation potentials and interpretation of the obtained data based on the analysis of elementary processes in the plasma.

2. EXPERIMENTAL

In this work, the intensities of the lines $J(t)$ and spectra emitted by a cylindrical dielectric barrier discharge (Fig. 1) were recorded using the multichannel photon counting method. The electrodes were strips of aluminum foil 5 cm wide located on both sides of the surface of the discharge tube along its entire length so that the gaps between them, which are necessary to prevent the electrical breakdown along the glass surface, were ≈1.2 cm. The change in the electron density of the plasma created by the circuit in Fig. 1 was achieved by adjusting the duration of the transistor-opening pulse T_p, i.e., the energy $Li^2/2$ (L is the inductance of the primary coil of the transformer, i is the current in this coil at the end of the pulse T_p). This energy is transferred to the secondary coil at the end of the pulse T_p in such a way that the current between the electrodes is two half-waves of different polarities with an amplitude of up to several hundred milliamperes and a duration of 2–3 μs each with a zero average value. The ratio of the numbers of turns N_2/N_1 was also selected depending on the gas pressure. Ring ferrite cores with an external diameter of 7.5 cm and permeability μ=30 were used as a magnetic circuit. It is obvious that the maximum voltage on the electrodes in the circuit under consideration is equal to the product $U_{max}N_2/N_1$ (U_{max} is the maximum permissible voltage on the transistor collector). In our experiments, we usually used IGBT transistors with $U_{max} = 600–1200$ V and transformers with a ratio $N_2/N_1 = 10–20$. These parameters were sufficient to create plasma with an electron density of $[e] \approx 10^{10}–5\times10^{11}$ cm^{-3} at a neon pressure from fractions to tens of torr. With regard to the average electron energy T_e (we use the term "electron temperature" in this sense, bearing in mind the possibility of a significant deviation of the electron energy distribution from the Maxwellian one in the active stage), for the purposes of this work we limit ourselves to indicating the fact of the appearance of doubly charged neon ions in the plasma in an amount sufficient to form a recombination spectrum that significantly exceeds the atomic spectrum in terms of luminous flux in the near ultraviolet region. In addition, we note that in the model solutions discussed below, the optimal (giving the best description of the experiment) T_e values were values approaching 100000 K). The discharge tube temperature did not exceed room temperature, i.e., no noticeable nonuniform heating of the gas occurred at energy inputs characteristic of the conditions of this work (fractions–units of watts depending on the discharge frequency). The experiments have shown that the discharge of the configuration discussed at pressures of ≈1 Torr creates an almost uniform plasma formation both along the cylinder axis and along the radius. The threadlike (streamer) character of the breakdown is manifested at pressures higher than 15 Torr. The thickness d of the discharge tube wall, i.e., the thickness of the dielectric layer at each electrode, was $d = 0.15$ cm. At the stage of plasma decay, electrons could be "heated" by a pulsed (in this work, the pulse duration was 1–2 μs) electric field of a high-frequency generator (RF in Fig. 1) connected to an inductance coil wound over the DBD electrodes. The time resolution of the recording circuit (the width of the counter channel) could vary within 40×2^k ns at $k = 0–15$ and the number of channels was 2048. Spectra, depending on the task, were recorded in the photon counter channels or with time resolution using an external pulse (strobe) $\Delta t_s \geq 1$ μs, synchronized with the pulse T_p of the discharge creation scheme (described in detail in

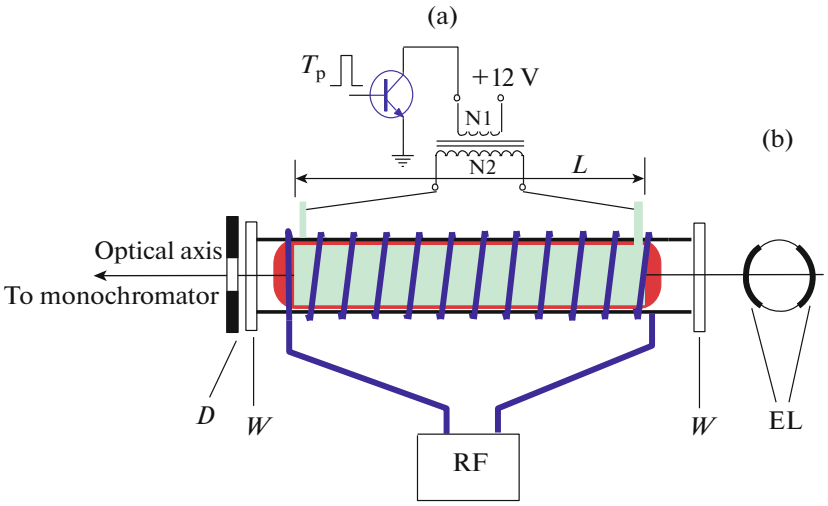

Fig. 1. (a) Scheme of the combination of barrier and pulsed high-frequency (RF) discharges in a 4 cm diameter glass tube, *D* is the 5-mm-diameter diaphragm, *W* are quartz windows; (b) arrangement of DBD electrodes on the surface of the discharge tube, $L = 20$ cm.

[1–3]), or integral over time. The spectrum was scanned by rotating the monochromator diffraction grating with an angular velocity determined by the signal level and the choice of the number of channels N_s in the spectrum. For example, at a plasma electron density in the center of the discharge tube $[e] \approx 10^{11}$ cm^{-3}, $N_s = 512$ and spectral resolution of $\Delta\lambda \approx 0.05$ nm the time of recording the time-integrated fragment of the spectrum with a width of $\Delta\lambda \approx 50$ nm in the near ultraviolet region filled with the brightest ion lines, was ≈1000 s. The density $[e]$ in the afterglow was estimated by the relaxation rate of the population of the resonance level Ne($2p^5 3s(^3P_1)$) after the pulsed disturbance by the RF discharge (RF in Fig. 1) with a duration of 1 μs in the initial stage of the recombination afterglow behind the maximum of the atomic line intensities. We estimate the accuracy of determining the electron density using this procedure at a level of 30% [3]. This $[e]$ value was used as the first approximation in processing the experimental data using the afterglow model [2] and was refined as the model solutions approached the measured intensities $J(t)$ of the spectral lines.

3. EXCITATION OF ION LINES IN THE DISCHARGE AND AFTERGLOW

Figure 2 shows the time dependences of the intensities $J(t)$ of several Ne^{+}* ion lines, which most clearly demonstrate the differences discussed below. The two intensity maxima at the beginning of the time scale correspond to the active stage of the discharge, which, as shown schematically in Fig. 1 (see above), is defined by two current half-waves differing slightly in duration [3]. During this phase, the intensities of all lines—both atomic and ionic—exhibit similar behavior, differing only in the depth of the "dip" between the maxima, which correlates with the excitation potentials of the corresponding levels. Significant differences in the evolution of the intensities emerge in the subsequent phases.

3.1. Excitation of Ion Lines in the Active Stage

The same as in [1, 2], we compare the intensities at characteristic points in time. Note that we have found no noticeable differences in the distribution of intensities over the spectrum at the maxima of the active stage, so we use the results of the measurements within the Δt_1 interval as data related to the discharge. In [2], we noted that the relative intensities of ion lines $J_i(\Delta t_1)$ correlate with the results of measurements [15] of the cross sections of the direct excitation by electrons of the beam discharge of the Ne^{+}* states from the ground state of the neon atom. Here we confirm this observation with experimental data. Table 1 presents the relations $J_{rel}(\Delta t_1)$ of the intensity of the brightest (2000 according to NIST [10]) 332.37 nm ion line to the intensities $J_i(\Delta t_1)$. Taking into account the multi-

Table 1. Ratio of the intensity of the 3323.7 nm line in the active stage (discharge) to the intensities of some of the brightest ion lines

λ_i, nm	E_h, eV	J_{NIST}	$J_{rel}(\Delta t_1)$ [2]	$J_{rel}(\Delta t_1)$, this work
333.48	30.885	400	8.2	6
335.50	30.927	400	10	8.5
336.06	30.958	400	25	16
337.82	31.520	1000	1.8	1.8

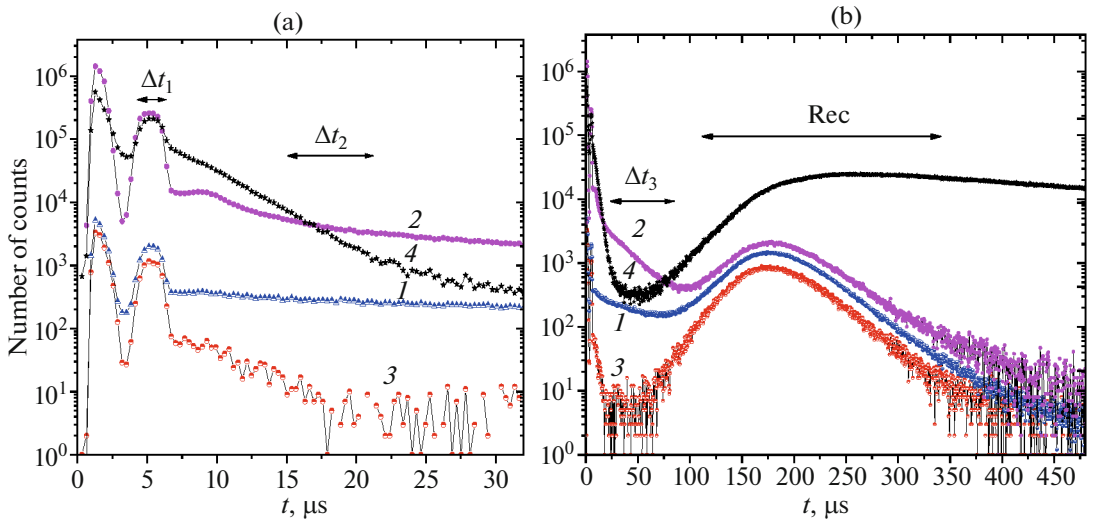

Fig. 2. Spectral line intensities in DBD plasma in neon. Pressure of 1.4 Torr, discharge frequency of 500 Hz, electron density at the beginning of the afterglow $[e] \approx 1.4 \times 10^{11}$ cm^{-3}; $t = 0$ is the beginning of the discharge. (a) Discharge and early afterglow, (b) the same data in the recombination stage; (*1*–*3*) are ion 321.82, 356.58, and 421.97 nm lines, respectively; (*4*) is the atomic 576.4 nm line.

ple changes in the relative intensities of all ion lines $J_i(t)$ over time in the active stage (see Fig. 2a), the data in Table 1 can be considered to be quite convincing.

The issue of the role of the excitation in the active stage from the ground state $^2P_{1/2,3/2}$ of the Ne^+ ion is resolved by setting up a simple experiment: the observation of the dependence $J_i(t)$ at essentially different frequencies F of the discharge (Fig. 3). The difference in the conditions for the discharge development is that at $F = 50$ Hz by the end of the afterglow t_{Max} the electron density $[e](t_{Max})$ (and, accordingly, the density of Ne^+ ions) drops by more than two orders of magnitude, whereas at 500 Hz it drops by about two times.

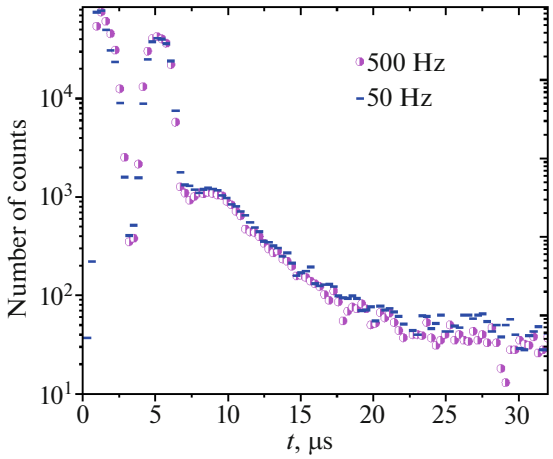

Fig. 3. Ion 332.37 nm line in DBD plasma at frequencies of 50 and 500 Hz. Conditions correspond to data in Fig. 2.

Qualitatively, this difference in electron densities follows from the dependence $J_a(t)$ of the 576.44 nm atomic line in the recombination stage of the afterglow (Fig. 4). The indicated changes in the quantity $[e](t_{Max})$ calculated using the model [16], which takes into account the electron density and temperature dependence of the rate constant of the collisional-radiative recombination of Ne^+ [17]. Figure 3 shows that the change in frequency by an order of magnitude leads to only a slight increase in the intensity of the 332.37 nm line, the same as other ion lines, i.e., it does not significantly complement the mechanism of the direct excitation with ionization. As the frequency further increases to 1500 Hz (the maximum value in our experiments), there was a slight change in the brightness of the lines at the maxima (higher in the second one) and its increase within one and a half times in the recombination stage of the afterglow, which indicates a slight increase in the densities of charged particles in a discharge with nonzero initial conditions for the electron density. At the same time, we observed no noticeable changes in the relative intensities of the lines Table 1, therefore, we consider the collision of the "fast" electron with an atom in the ground state as the main excitation mechanism in the discharge

$$Ne + e \rightarrow Ne^{+*} + e + e. \quad (1)$$

3.2. Excitation of Ion Lines in the Early Afterglow

Figure 2 shows that the character of the change in the ion lines in the afterglow preceding the recombination one, firstly, differs dramatically from the $J_a(t)$ of lines of the atomic spectrum, the brightness decline

of which is due to the relaxation of the average electron energy (T_e) forming the flow of the stepwise excitation from the metastable states of the neon atom of the $2p^5 3s$ configuration [1] after the second maximum (Fig. 2a), and secondly, indicates the presence of three groups of lines reflecting the manifestation of different mechanisms of the population of ion levels at this stage. In [2], the results of our experiment with pulsed "heating" of electrons showed the absence of a response of the intensities of the group of lines, which in Fig. 2 is represented by the 321.82 nm line (we designate this group as $J_{i1}(t)$), to an increase in T_e in the interval of Δt_2. We suggested that at this stage their excitation is not associated with plasma electrons, but occurs with the participation of only heavy particles. The difference in the excitation energies E_h of the upper levels of this group of lines reaches almost 4 eV but, in addition, the following difference takes place between them: the lines with small E_h (the brightest of them in the sensitivity region of the measurement scheme is 333.48 nm, Table 1) can be matched with cascade "donors" that fill them with their transitions [2] from levels with energies $E_h \approx 34.7$ eV. In particular, one of such donors of the 333.48 nm line is the 321.82 nm line. The latter, if they manage to find similar donors (e.g., 439.2 nm (transition $4f \rightarrow 3d$) for the 321.2 nm line), then only those that do not possess the discussed feature. The typical behavior of the $4f$-level populations is presented in Fig. 2 by the 421.97 nm line. The set of ion lines studied and significantly expanded in this work and experiments with electron "heating" (some results are shown in Fig. 5) confirms the hypothesis about the origin of the ion line glow at the discussed intermediate stage that is not related to electrons. The absence of the stepwise excitation stage characteristic of atomic lines corresponds to conclusions of [11, 12] about the absence of metastable excited states of the neon ion with lifetimes exceeding 10 μs mentioned in the introduction. Thus, it can be assumed that the total energy of heavy particles of the desired reaction, populating mainly the ion levels of the $2s^2 2p^4(^3P)3d$ and $2s^2 2p^4(^3P)4s$ configurations with energies of 34.5–35 eV, should be no less than 35 eV, but, on the other hand, insufficient for the excitation of $4f$ levels (Table 2), thereby ensuring the threshold nature of the excitation. As an example of such a reaction, we propose to consider a collision involving the following particles:

$$\mathrm{Ne}^{2+}\left(^3P\right) + \mathrm{Ne}_m \rightarrow \mathrm{Ne}^{+} + \mathrm{Ne}^{+*}, \qquad (2)$$

where $\mathrm{Ne}^{2+}(^3P)$ is the ion in the $^3P_{0,1,2}$ ground state (the distance between sublevels in the energy scale is about 0.1 eV), Ne_m is a neon atom in the metastable $^3P_2$ state of the $2p^5 3s$ configuration. The total energy of particles in the input channel (2) is (21.56 + 41.08) + 16.62 = 78.98 eV (21.56 and 41.08 are ionization energies of the neon atom and neon ion), on the left-hand side 21.56 + (21.56 + E_{th}), from where for the maximum excitation energy of the ion on the right-hand side of Eq. (2) we obtain $E_{1th} \approx 36$ eV. Note that fairly high rate constants exceeding 10^{-14} cm^3/s correspond to reactions similar to Eq. (2) involving atoms in the input channel in the ground state [18]. It is obvious that reactions involving a metastable atom should be more effective because of the polarization character of the interaction of particles at such a high polarizability (186 at. units) as the Ne_m atom has [19]. The authors of [20] consider a similar process in the helium plasma as one of the main mechanisms of the destruction of the He^{++} ion; cross sections significantly exceeding 10^{-15} cm^2 correspond to similar reactions of the ion transformation involving hydrogen atoms (deuterium) interacting with Ne^{3+} at thermal energies [21].

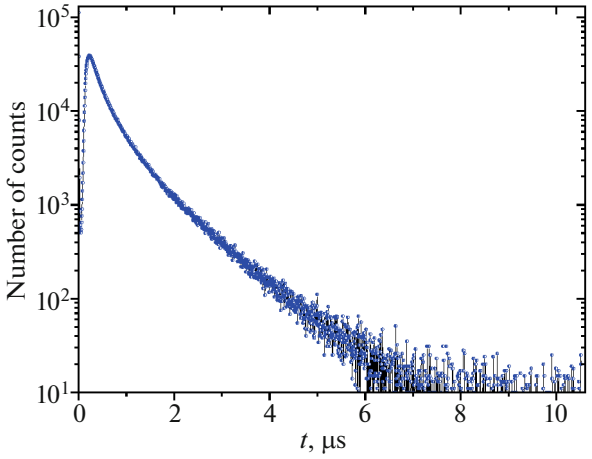

Fig. 4. Intensity of the atomic line at 576.4 nm at a discharge frequency of 50 Hz. The conditions correspond to the data in Fig. 2.

The analysis of a large number of relatively weak lines performed in this work made it possible to detect

Table 2. Excitation energies of levels and transitions for ion lines discussed in the text

λ, nm	Transition	E_h, eV	NIST intensity
296.72	$4s \rightarrow 3p$	38.2	300
321.82	$3d \rightarrow 3p$	34.73	300
322.95	$3d \rightarrow 3p$	37.8604	180
322.96	$3d \rightarrow 3p$	37.8603	240
3323.7	$3p \rightarrow 3s$	31.51	2000
333.48	$3p \rightarrow 3s$	30.88	400
356.85	$3d \rightarrow 3p$	34.02	500
421.97	$4f \rightarrow 3d$	37.55	300
4392.0	$4f \rightarrow 3d$	37.56	400

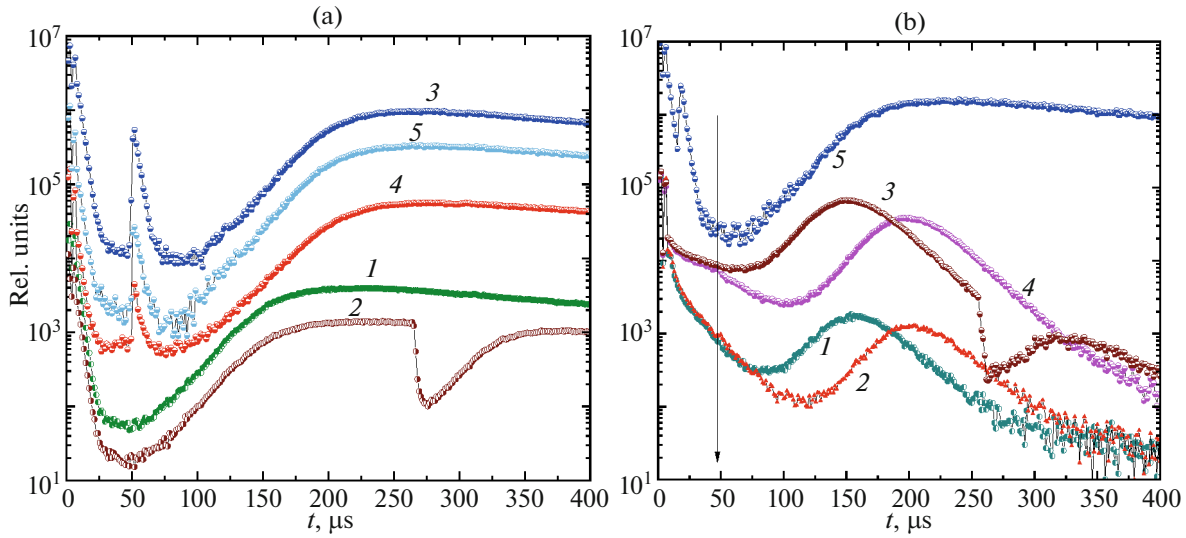

Fig. 5. Reaction of the intensities of atomic and ionic lines in the afterglow to pulsed "heating" of electrons by the RF field. Neon pressure of 1.7 Torr, electron density at the beginning of the afterglow $[e] \approx 1.8 \times 10^{11}$ cm^{-3}: (*1*–*3*) line at 576.42 nm ($4d \rightarrow 3p$), (*4*, *5*) line at 486.55 ($6d \rightarrow 3p$); voltage $V_{RF} = 0$ (*1*), 50 (*2*), 250 (*4*) and 280 V (*3*, *5*) (a); ion line 356.58 (*1*, *2*) and 333.48 nm (*3*, *4*, *5*) atomic line at 576.42 nm; $V_{RF} = 0$ (*1*), 50 (*3*), 280 V (*2*, *4*, *5*) (b). The arrow indicates the position of the RF pulse start for (*2*, *4*). The data are shifted vertically for ease of observation.

one more group of lines (we denote it as $J_{i2}(t)$), the brightest of which, at 356.85 nm, is presented in Table 2, Figs. 2b and 5b. The emission of these lines in the afterglow region under discussion decreases noticeably faster than $J_{i1}(t)$ and can exceed the recombination emission in intensity. The same as in the case of the first group, the source of emission of the brightest of them are transitions from excited states with the energies of 34–35 eV. However, there is a fundamental difference: for the $J_{i2}(t)$ lines, it is possible to find cascade donors emitted by levels with energies noticeably exceeding the E_{1th} found above. As an example, we indicated three such donors of the 356.85 nm line: 322.95, 322.96, and 296.72 nm in Table 2. Their behavior under all conditions in the afterglow was identical to that of the 356.85 nm line. Therefore, to interpret $J_{i2}(t)$, it is necessary to supplement the reaction (2) with a similar one, but with the energy of the particles such that $E_{2th} \approx 38$ eV.

Turning to reaction (2) to explain the results of the experiment, it is logical to consider the participation of two other states of the Ne^{2+} ion of the $2s^2 2p^4$ configuration, $^1D_2$ and $^1S_0$, in it, and for satisfying the condition $E_{2th} \geq 38$ eV it is enough to turn to the state $^1D_2$ whose energy exceeds $^3P_{0,1,2}$ by 3.3 eV:

$$Ne^{2+}(^1D_2) + Ne_m \rightarrow Ne^+ + Ne^{+*}. \quad (3)$$

In our experiment, there is no instrument for tracking the ion densities in different states. We can only assume that the energy difference of 3.3 eV against the background of more than 60 eV required for the appearance of doubly charged ions in neon plasma is small enough to be able to estimate the ratio of ion densities from the statistical weights of the states $[Ne^{2+}(^1D_2)]/[Ne^{2+}(^3P_{0,1,2})] = 5/9$.

Let us discuss in more detail the behavior of atomic and ion lines in the afterglow with a pulsed RF field according to the data in Figs. 5 and 6. By moving the RF field pulse from the region of recombination glow to the origin (Fig. 5) and repeatedly increasing its amplitude, on all atomic lines (measurements were carried out up to the lines of transitions $9d$–$3p$) a distinct reaction could be observed—a sharp increase in intensities to values characteristic of the region of the stepwise excitation in the early afterglow. At the same time, only a slightly increased decay rate of $J_{i1,2}(t)$ and similar to $J_a(t)$ shift of the maximum of recombination luminescence due to expansion of the region with increased electron temperature can be observed on ionic ones. Note that this level of RF field amplitude was sufficient to initiate a steady-state RF discharge. Finally, the third group of ion lines J_{i3} is lines without the intermediate stage typical for J_{i1} and J_{i2}. This group includes, in particular, all lines of $4f \rightarrow 3d$ transitions, whose response to the pulsed RF field at this stage is also limited by the shift of the maximum in the afterglow.

A "splash" of atomic line intensities similar to that shown in Fig. 5a can be obtained directly in the region of stepwise excitation, bringing the RF field pulse closer to the second maximum $J_a(t)$ in the discharge (Fig. 5b). In this case, the expected approach of the

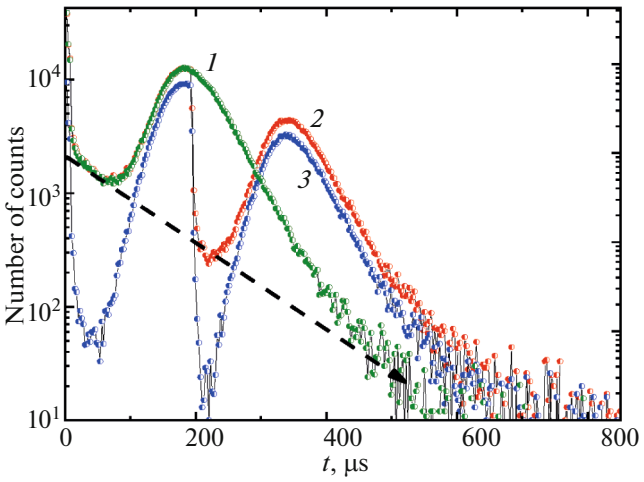

Fig. 6. Afterglow of the lines of the first ((*1*, *2*) 333.48 nm) and third ((*3*) 439.2 nm) groups. The electron density at the beginning of the afterglow $[e] \approx 1.1 \times 10^{11}$ cm^{-3}. The dashed line is the estimated contribution to the intensity $J_{i1}(t)$ of the process Eq. (2).

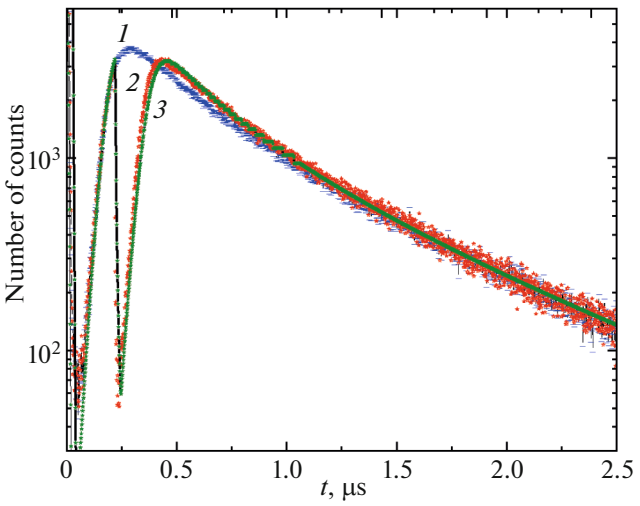

Fig. 7. Recombination stage of afterglows of the line (*1*) 576.4 nm, (*2*) $J_{576.4}(t)$ with pulsed "heating" by RF discharge; (*3*) model solution. Electron density at the beginning of the afterglow $[e] \approx 1.1 \times 10^{11}$ cm^{-3}, neon pressure of 1.4 Torr.

recombination luminescence maximum to the position corresponding to curve *1* (Fig. 5a) is observed, since the disturbance introduced by the RF field becomes small compared to the average energy of the electrons created by the discharge. The growth of the intensities of the ion lines was not observed in this case as well.

The results of a series of experiments with RF heating of electrons are shown in Figs. 6–9. The first of them shows the suppression of the recombination radiation in the afterglow stage on the ion lines of the first and third groups. With the characteristic for collisional-radiative recombination dependence of the rate constant of the process $\alpha(T_e) \sim T_e^{-9/2}$ it is enough to superimpose a small RF field on the afterglow, the level of which is easy to select, to suppress the glow of the lines of the third group almost to a dark background. In this case, the intensity J_{i1} respond to heating by a significantly smaller drop, dropping to the level $J_x(t)$, which is determined by the desired process involving heavy particles. A similar difference is observed when comparing the intensities J_{i2} and J_{i3}. By moving the time of heating of electrons, it is easy to record in such an experiment the change of $J_x(t)$ over a wide time interval, which simplifies the comparison $J_x(t)$ with the change in the afterglow of the densities of the supposed participants in the collisions Eqs. (2) and (3).

Let us consider the kinetics of Ne^{2+} ions in the plasma decay stage. In our experiment, which does not have a direct instrument for measuring the density of doubly charged ions, information about $[Ne^{2+}](t)$ can be obtained on the basis of a model of processes in the decaying neon plasma [16], describing the evolution of densities of Ne^{2+}, Ne^+, Ne_2^+ ions, electrons $[e] = [Ne^+] + [Ne_2^+] + 2[Ne^{2+}]$ and temperature T_e taking into account the most significant elementary processes. The appeal to the afterglow model, capturing also the recombination stage (Figs. 7 and 8), requires substantiation of the applicability of using as a criterion of adequacy of the model the coincidence of its solutions with the experimental dependences $J(t)$ of the spectral lines used in the work. Such substantiation should indicate the proportionality of the line intensities to the flows of the collisional-radiative recombination of the ions under consideration with plasma electrons. With respect to singly charged ions,

$$Ne^+ + e + e \xrightarrow{\alpha_{1cr}} Ne^* + e \qquad (4)$$

the problem is solved relatively simply: at the electron density of $[e] \approx 10^{11}$ cm^{-3} the purely collisional model of process (4), within which his theory [22] was constructed, which relates the recombination rate to the relaxation flux of the excited electron in the right-hand side of Eq. (4) in collisions with plasma electrons, is applicable only for highly excited (Rydberg) states of atoms, whereas in the region of states with small principal quantum numbers the recombination flux is transferred by radiative transitions. As such, we use one of the $4d \to 3p$ transitions, which gives the 576.4 nm line, assuming that $J_{576.4}(t) \sim \alpha_{1cr}[Ne^+][e]^2$ and in the kinetics of $4d$ levels, collisional transitions play a minor role compared to radiation. This choice can be justified by referring to known estimates [23, 24], or by using the experimental results directly,

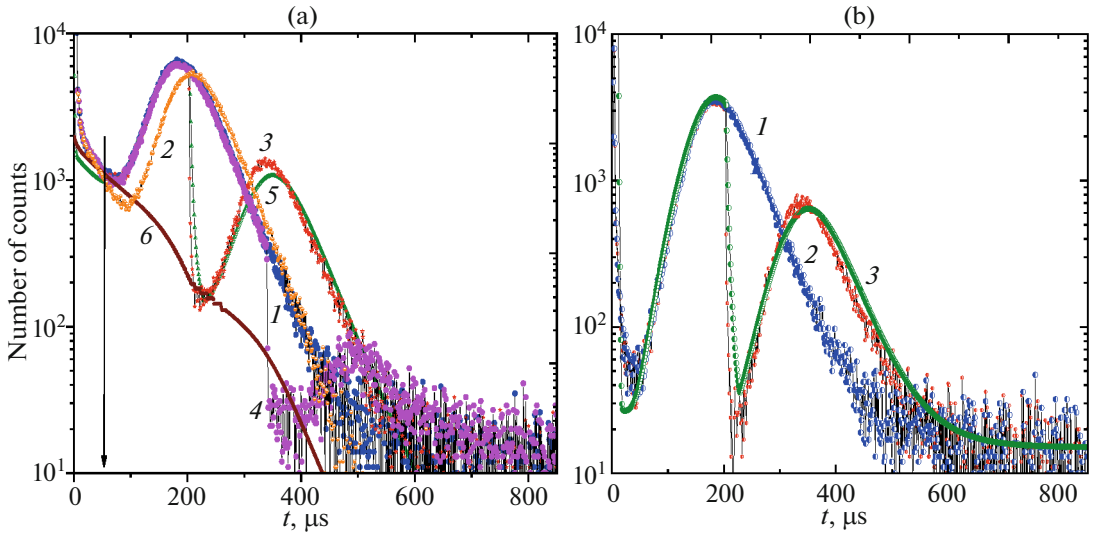

Fig. 8. Model $J_M(t)$ solutions and experimental intensities of ion lines. The conditions are the same as in Fig. 6. For the 333.48 nm line (a): (*1*) without heating the electrons, (*2–4*) with pulse heating at a voltage of 100 V on the inductor. The arrow shows the position of the RF pulse for the case *2*; (*5*) $J_{M1}(t)$ for the group $J_{i1}(t)$, (*6*) density $[Ne^{2+}](t)$ normalized to $J_{M1}(t)$ at time t indicated with an arrow; for the 439.2 nm line (b): (*1*) without RF, (*3*) $J_{M3}(t)$ for the group of lines $J_{i3}(t)$ (*2*).

comparing $J_{576.4}(t)$ with a series of line intensity measurements $J_n(t)$, increasing the principal quantum number n. The same as in [5], we were able to record quantum fluxes in lines up to $n = 9$ (the 439.5 nm line, the bond energy ε* of the excited electron of 0.16 eV). The measurements showed that $J_{576.4}(t)$ and $J_n(t)$ are close up to $n = 7$, and the behavior $J_{439.5}(t)$ was significantly closer to the corresponding equilibrium of the population of the 9*d* level with the continuum than to $J_{576.4}(t) \sim \alpha_{1cr}[Ne^+][e]^2$.

In relation to ion lines, similar [23, 24] criteria are unknown to us, therefore the correspondence of intensities to the recombination flow of doubly charged ions $J_i(t) \sim \alpha_{2cr}[Ne^{2+}][e]^2$ we attribute this to the fact that in the recombination stage of the afterglow, all observed lines, regardless of the binding energy ε* (the minimum ε* value is more than 3 eV), behaved identically.

The ion lines were simulated in two stages. The first stage was to describe the recombination glow of the 576.4 nm line based on literature data on the main processes that determine the plasma parameters and the density of the particles under consideration. In this case, the dependence of the collisional-radiative recombination coefficient α_{1cr} on these parameters was set by the formula

$$\alpha_{1cr} = 1.55\times10^{-10}T_e^{-0.63} + 6.0\times10^{-9}T_e^{-2.18}[e]^{0.37} + 3.8\times10^{-9}T_e^{-4.5}[e], \quad (5)$$

proposed by the authors [17] to describe the recombination of atomic ions in a wide range of plasma electron densities. The initial conditions for the system of differential equations of the model [16] were the values of the densities of charged and long-lived excited particles of the $2p^53s$ configuration, giving a solution corresponding to their experimentally determined reference values: as mentioned above, the electron density was estimated from the response of the population of the $^3P_1$ level to the pulsed heating of electrons, the population $[^3P_0](t)$, $[^3P_1](t)$ and $[^3P_2](t)$ were measured by the absorption method in the entire afterglow. The electron temperature at the end of the active stage was selected in the first approximation from the condition of the best description of $J_{576.4}(t)$ from the beginning of the recombination stage. As an example, Fig. 7 shows such a solution. Note the characteristic increase in intensity due to the heating of the electrons after their "cooling," which occurred for all lines associated with processes (1) and (4). This phenomenon, caused by the suppression of collisional-radiative recombination during the relaxation time of the electron temperature and significantly more pronounced in the ion spectrum (Fig. 6), was used by us [6] to determine the ratio of the recombination coefficients $\alpha_{2cr}/\alpha_{1cr}$. It is important that the result is quite obvious simply from a comparison of the experimental data and does not require recourse to the afterglow model, thereby eliminating doubts about its adequacy.

As for the assignment of initial ion densities, for pressures on the order of 1 Torr it is easy to justify the relation $[Ne_2^+](t = 0) = [Ne^+](t = 0)$, since the rate constants of processes involving them have been measured many times. With doubly charged Ne^{2+} ions it is

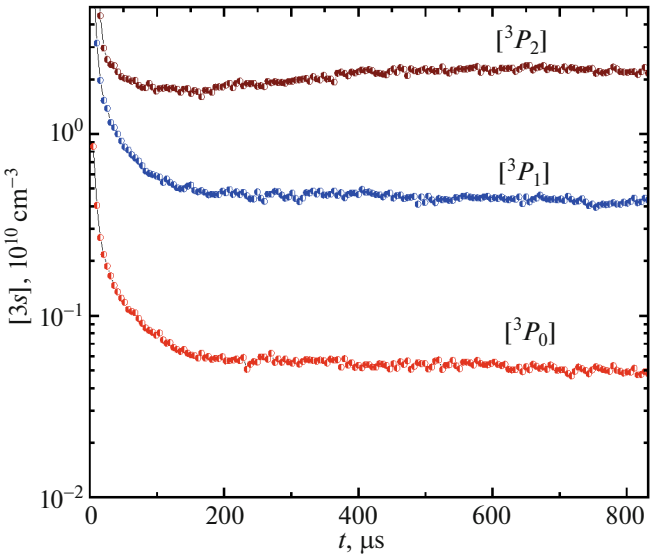

Fig. 9. Populations of the $2p^5 3s$ configuration levels. The conditions are identical to those in Figs. 7 and 8. At the end of the discharge, $[^3P_2] = 1.2\times10^{11}$, $[^3P_1] = 0.8\times10^{11}$, and $[^3P_0] = 0.12\times10^{11}$ cm^{-3}.

more complicated, because until recently their kinetics in plasma remained outside the attention of researchers. Generally speaking, the afterglow of both ion and atomic lines depends on the density ratio $([Ne^{2+}]/([Ne^+])(t = 0)$, since both of them, firstly, carry away electrons due to Eqs. (1) and (4), and Ne^{2+} significantly faster [6], and, secondly, their densities are related by the conversion process [18, 25]

$$Ne^{2+} + Ne \rightarrow Ne^+ + Ne^+. \quad (6)$$

By varying the ratio of ion densities during the simulation of ion line intensities $J_i(t)$ we have repeatedly observed changes in the model $J_M(t)$ curves towards $J_i(t)$. However, in this multiparameter problem with such a strong dependence of the solution on the electron temperature (according to [22] $J_M(t) \sim T_e^{-4.5}$) and the uncertainty of some of them (the data [18, 25] on the reaction rate constant (6) diverge by a factor of three, the frequency of electron–ion collisions in the equation for $T_e(t)$ is calculated approximately, etc.) it was possible to obtain a similar result by a small change within reasonable limits of other parameters. Therefore, without having other grounds, the initial density $[Ne^{2+}]$ was set such that the solution practically did not depend on it, which was carried out when $[Ne^{2+}]/([Ne^+])(t = 0) < 0.05$. As one of the main parameters of the problem, the ratio of the rate constants of collisional-radiative recombination Eqs. (4) and (1), we used the value found by us in the above-mentioned experiments [6] $\alpha_{2cr}/\alpha_{1cr} = 21$, which is almost three times higher than the value predicted in [22] $\alpha_{2cr}/\alpha_{1cr} \sim Z^3$ (Z is the ion charge).

Some results of the simulation $J_M(t)$ are presented in Fig. 8. They show that within the model under consideration it is possible to qualitatively interpret the experimental data. In addition to the intensities, Fig. 8 shows the solution for the ion density $[Ne^{2+}](t)$ (the initial value in the model $[Ne^{2+}](t = 0) = 0.05$ at the density $[Ne^+](t = 0) = 1.3\times10^{11}$ cm^{-3}). The densities of metastable atoms required for constructing the excitation flux in the process Eq. (2) are shown in Fig. 9. The measurements were carried out using the relative absorption method with recording the discharge radiation in neon at a pressure of 1 Torr in a tube with a diameter of 1.5 cm located as shown in Fig. 1b. The relative absorption measurements were processed under the assumption of the same Doppler character of the broadening of the spectral lines in both tubes. To minimize errors associated with the possible uncertainty of the character of broadening, spectral lines with close integral absorption coefficients were selected: 614.7 nm for the state $^3P_2$, 607.4—$^3P_1$, 626.6—$^3P_0$. In order not to introduce additional uncertainty, although there is a small but noticeable difference between the experimental and model curves for the population of these states, and taking into account their weak dependence on time after the initial decline, for comparing the product $[Ne^{2+}][^3P_2]$ (in the process Eq. (2)) we propose to consider the model solution of Fig. 8a, correlating it with the data of Fig. 9. In our opinion, the result of such a comparison justifies the assumption about process Eq. (2) as a source of the population of a significant number of excited levels of the neon ion. In this model, the acceleration of the decay of the intensities of the lines of the

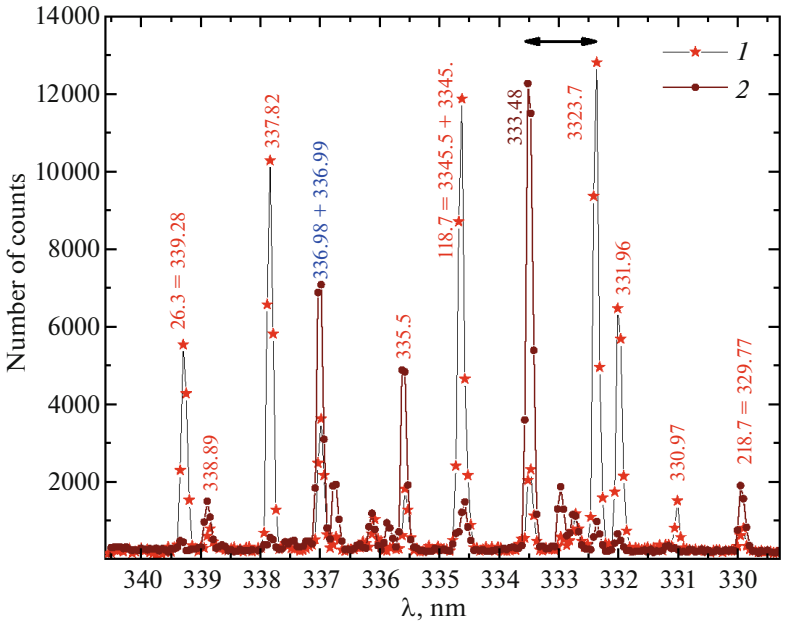

Fig. 10. Spectra emitted in the active stage (*1*) and recombination afterglow (*2*). For ease of comparison, the intensity maxima of the 332.37 and 333.48 nm lines (shown by arrows) are superimposed.

group J_{i1} observed in the experiment with RF heating of electrons can also be explained (data Eq. (2) Fig. 8a): the effect is due to an increase in the ambipolar diffusion rate of the Ne^{2+} ion and expected acceleration of decay $[^3P_2](t)$ [26].

It is more difficult to justify the participation of $Ne^{2+}(^1D_2)$ ions in reaction Eq. (3). At present, as far as we know, there are no data on the kinetics of $Ne^{2+}(^1D_2)$ ions in the plasma, with the exception of their ambipolar diffusion [27] and conversion Eq. (6) during collisions with atoms. Therefore, reaction Eq. (3) remains a hypothesis not confirmed for now by comparison with experimental data. One can only assume that the accelerated decline in comparison with the lines of the first group $J_{i2}(t)$ in the afterglow stage Δt_3 is associated with the participation of excited neon atoms $2p^53s(^3P_1, {}^3P_0)$ in Eq. (3), the densities of which (Fig. 9) vary significantly faster than $[^3P_2]$, as well as with the possible relaxation of the population of $Ne^{2+}(^1D_2)$ to the ground state during collisions with plasma particles.

The following should be added to the discussion of the model's compliance with the experimental conditions. The model disregards the changes over time in the radial distribution of the densities $N(r)$ of charged and excited particles, which is created by the barrier discharge of the configuration under consideration with a "dip" in the center of the tube, clearly expressed at pressures of tens of torr [28] and persisting for a long time during the plasma decay stage. However, at low pressures, the initial distribution, close to the Π-shaped one, quickly (at $P \approx 1$ Torr in 20–30 μs [29]) comes to the Bessel distribution due to higher diffusion modes. We checked the possible influence of the change in $N(r)$ on the course of the intensities $J(t)$ by comparing the radiation of the discussed DBD with a longitudinal discharge in the same tube, replacing the side electrodes with ring electrodes 1 cm wide at a distance of $L = 20$ cm. Measurements performed with the same parameters of the power supply circuit indicated the following differences: the intensities of the ion lines in the longitudinal discharge are approximately twice as weak as in the transverse discharge, the active stage has noticeably shortened (apparently due to a decrease in the capacitance of the electrodes), a weak longitudinal inhomogeneity of the plasma glow has appeared, depending on the polarity of the electrodes, the aforementioned small "dip" in the intensities of the lines and the density $[^3P_2]$ in the Δt_2 stage (Fig. 2) is absent. We find no significant discrepancies between the model solutions and the measurement results; solutions in the model similar to those presented in Figs. 8 and 9 were obtained by simply selecting reduced initial densities of charged particles.

In conclusion of the discussion of the ion line intensities of the barrier discharge plasma, we note one unexpected, in our opinion, phenomenon, which is obvious when referring to the spectra (Fig. 10) measured with time resolution in the stages of discharge (Δt_1) and recombination afterglow Rec. It is most clearly manifested when comparing the intensities of the brightest (according to NIST $J = 2000$) 332.37 nm line (the upper level energy of 31.512 eV) with other ion

lines discussed in the work, e.g., with the similar 333.48 nm line in spectrum ($J = 400$, 30.885 eV). In the discharge stage $J_{332.37} \gg J_{333.48}$ (Table 1), while its recombination glow is much less intense (Fig. 10). Some other bright lines behave similarly, e.g., 337.82 ($J = 1000$) and 330.97 ($J = 300$) emitted by the level of 31.528 eV close to 31.512 eV. Moreover, all of those discussed belong to the same electron configuration $2s^2 2p^4 (^3P) 3p$. Taking into account the fact that the population of the level 31.512 eV is formed, the same as 30.885 eV, by transitions from more than 20 excited levels of the ion, we find it difficult to explain such a "dip" in the recombination flow to the indicated levels. A similar effect is not observed in the atomic spectrum (in Fig. 10 it is represented by a doublet 336.98 and 336.99 nm, transition of $4p \rightarrow 3s$).

4. CONCLISIONS

In this work, kinetic spectroscopy methods are used to study the time dependences of the ion line intensities of low-frequency dielectric barrier discharge plasma in low-pressure neon and their response to pulsed "heating" of electrons by a high-frequency discharge at different stages of the afterglow. The comparison of the experimental results, supplemented by measurements by the absorption method of populations of excited levels of the $2p^5 3s$ configuration of the neon atom, with model solutions made it possible to explain the laws of the evolution of plasma radiation in the ion spectrum. Transition from the stage of plasma creation (discharge) with the population of all excited levels of the Ne^{+*} ion from the ground state of the atom to the recombination afterglow, unlike the atomic spectrum, does not contain a stepwise excitation stage. At this intermediate stage, ion radiation, which does not respond to the high-frequency field, is represented by three groups of lines depending on the energy of the excited state. The first and second groups are filled with lines with energies of the upper levels less than 35 eV and about 38 eV, respectively (counted from the ground state of the ion), with distinctly different characters of the decrease in intensity over time. The threshold character of the excitation of these lines is proposed to be attributed to the reaction $Ne^{2+} + Ne_m^* \rightarrow Ne^+ + Ne^{+*}$ involving neon atoms Ne_m^* in long-lived states $2p^5 3s$. The third group, which has no distinct intermediate stage, is represented in the work by transitions $4f \rightarrow 3d$ from $4f$ levels with energies ≈37.5 eV. At the recombination stage, all observed lines had the same afterglow character, caused by the collisional-radiative recombination of doubly charged ions with electrons with a characteristic for this process response of intensities to a small heating of electrons by a pulsed RF field, corresponding to the temperature dependence of the rate constant of the process $\sim T_e^{-4.5}$. Suppression of recombination glow by increasing the amplitude of the heating pulse made it possible to discover a new source of population of excited levels of neon ions in the plasma decay stage.

FUNDING

This work was supported by ongoing institutional funding. No additional grants to carry out or direct this particular research were obtained.

CONFLICT OF INTEREST

The author of this work declares that he has no conflicts of interest.

REFERENCES

1. V. A. Ivanov and Yu. E. Skoblo, Zh. Eksp. Teor. Fiz. **166**, 434 (2024). https://doi.org/10.31857/S004445102409013X
2. V. A. Ivanov, Zh. Eksp. Teor. Fiz. **167**, 893 (2025). https://doi.org/10.31857/S0044451025060161
3. V. A. Ivanov, Plasma Sources Sci. Technol. **2**, 045022 (2020). https://doi.org/10.1088/1361-6595/ab7f4c
4. V. A. Ivanov, Opt. Spektrosk. **131**, 1114 (2023). https://doi.org/10.21883/OS.2023.09.56602.5307-23
5. V. A. Ivanov, Opt. Spectrosc. **130**, 818 (2022). https://doi.org/10.21883/OS.2022.07.52719.3077-21
6. V. A. Ivanov, Opt. Spectrosc. **131**, 1469 (2023). https://doi.org/10.61011/EOS.2023.11.58042.5370-23
7. S. Frisch, Z. Phys. **64**, 499 (1930).
8. W. Persson, Phys. Scr. **3**, 133 (1971).
9. A. E. Kramida and G. Nave, Eur. Phys. J. D **37**, 1 (2006).
10. NIST Atomic Spectra Database Lines Form. https://physics.nist.gov/PhysRefData/ASD/lines form.html. Cited March 10, 2025.
11. H. D. Hagstrum, Phys. Rev. **104**, 309 (1956).
12. Z. Z. Latypov, S. E. Kupriyanov, and N. N. Tunitskii, Sov. Phys. JETP **19**, 570 (1964).
13. D. A. Church, Phys. Scr. **1995** (T59), 216 (1995).
14. R. Steinbrügge, S. Kühn, F. Nicastro, M. F. Gu, M. Togawa, M. Hoesch, J. Seltmann, I. Sergeev, F. Trinter, S. Bernitt, C. Shah, M. A. Leutenegger, and J. R. Crespo López-Urrutia, Astrophys. J. **941**, 188 (2022). https://doi.org/10.3847/1538-4357/ac9c00
15. K. G. Walker and R. M. St. John, Phys. Rev. A: At., Mol., Opt. Phys. **6**, 240 (1972).
16. V. A. Ivanov, Opt. Spectrosc. **129**, 992 (2021). https://doi.org/10.21883/OS.2021.08.51193.1987-21
17. J. Stevefelt, J. Boulmer, and J.-F. Delpech, Phys. Rev. A: At., Mol., Opt. Phys. **12**, 1246 (1975).
18. R. Johnsen and M A. Biondi, Phys. Rev. A: At., Mol., Opt. Phys. **18**, 996 (1978).
19. A. A. Radtsig and B. M. Smirnov, *Parameters of Atoms and Atomic Ions* (Energoatomizdat, Moscow, 1986) [in Russian].

20. O. V. Zhigalov, Yu. A. Piotrovskii, and Yu. A. Tolmachev, Opt. Spectrosc. **97**, 673 (2004). https://doi.org/10.1134/1.1828614

21. C. C. Havener and R. Rejoub, AIP Conf. Proc. **730**, 235 (2004). https://doi.org/10.1063/1.1824874

22. A. V. Gurevich and L. P. Pitaevskii, Sov. Phys. JETP **19**, 870 (1964).

23. L. M. Biberman, V. S. Vorob'ev, and I. T. Yakubov, *Kinetics of Nonequilibrium Low-Temperature Plasmas* (Nauka, Moscow, 1982; Consultants Bureau, New York, 1987).

24. P. Mansbach and J. Keck, Phys. Rev. **181**, 275 (1969).

25. F. J. de Hoog and H. J. Oskam, J. Appl. Phys. **44**, 3496 (1973).

26. V. A. Ivanov, J. Phys. B: At., Mol. Opt. Phys. **31**, 1765 (1998).

27. R. Johnsen and M A. Biondi, Phys. Rev. A: At., Mol., Opt. Phys. **20**, 221 (1979).

28. V. A. Ivanov, Opt. Spectrosc. **126**, 167 (2019). https://doi.org/10.1134/S0030400X1903007X

29. V. A. Ivanov, Opt. Spectrosc. **130**, 799 (2022). https://doi.org/10.21883/EOS.2022.07.54719.3076-21

Translated by L. Mosina